# Dynamic Transition Associated with the Thermal Denaturation of a Small Beta Protein

Daniela Russo,* Javier Pérez,† Jean-Marc Zanotti,* Michel Desmadril,‡ and Dominique Durand†

*Laboratoire Léon Brillouin, CE Saclay, 91191 Gif-sur-Yvette Cédex, †Laboratoire pour l'Utilisation du Rayonnement Electromagnétique, Université Paris-Sud, 91898 Orsay Cédex, and ‡Laboratoire de Modélisation et d'Ingéniere des Protéines, Université Paris-Sud, 91405 Orsay Cédex, France

ABSTRACT We studied the temperature dependence of the picosecond internal dynamics of an all-$\beta$ protein, neocarzinostatin, by incoherent quasielastic neutron scattering. Measurements were made between 20°C and 71°C in heavy water solution. At 20°C, only 33% of the nonexchanged hydrogen atoms show detectable dynamics, a number very close to the fraction of protons involved in the side chains of random coil structures, therefore suggesting a rigid structure in which the only detectable diffusive movements are those involving the side chains of random coil structures. At 61.8°C, although the protein structure is still native, slight dynamic changes are detected that could reflect enhanced backbone and $\beta$-sheet side-chain motions at this higher temperature. Conversely, all internal dynamics parameters (amplitude of diffusive motions, fraction of immobile scatterers, mean-squared vibration amplitude) rapidly change during heat-induced unfolding, indicating a major loss of rigidity of the $\beta$-sandwich structure. The number of protons with diffusive motion increases markedly, whereas the volume occupied by the diffusive motion of protons is reduced. At the half-transition temperature ($T$ = 71°C) most of backbone and $\beta$-sheet side-chain hydrogen atoms are involved in picosecond dynamics.

## INTRODUCTION

One of the challenges facing molecular biology is determining the rules that govern the acquisition by a nascent polypeptide chain of its three-dimensional and functional structure. Rapid progress in genome sequencing has made it all the more urgent to solve this problem. However, although protein folding is an extremely active field of research combining aspects of biology, chemistry, biochemistry, computer science, and physics, the detailed mechanisms of folding are not entirely clear (for a review see Brockwell et al., 2000, and references therein). A complete understanding of protein folding requires the physical characterization of both native and denatured states and evaluation of the thermodynamic parameters of the system. This involves obtaining information concerning the structure and dynamics of proteins denatured under various conditions. Over the last ten years or so, a large amount of structural information has been obtained experimentally on unfolded proteins, using various techniques including circular dichroism, fluorescence, nuclear magnetic resonance (NMR), small-angle x-ray, or neutron scattering. In contrast, much less attention has been paid to describing the dynamic properties of the denatured state. The main results obtained come mainly from NMR experiments with $^{15}N$ relaxation (Tollinger et al., 2001; Barbar et al., 2001; Bai et al., 2001; Yao et al., 2001) and molecular dynamic simulations combined with NMR (Wong et al., 2000).

In recent years, incoherent quasielastic neutron scattering (IQENS) has been used to describe the internal dynamics of proteins (for a review, see Smith, 2000). IQENS directly probes the internal dynamics of biomolecules on the picosecond time scale, providing information on diffusive motions and the geometry of the motions observed (Bée, 1988). These two components change significantly during denaturation. IQENS is a dynamic technique complementary to NMR and molecular dynamic simulation (Dellerue et al., 2001). This technique has already been applied to studies of the internal dynamics of native-state proteins (Réat et al., 1997, 1998; Fitter et al., 1998; Lehnert et al., 1998; Zaccai, 2000) focusing on the characterization of the dynamical transition around 180–200 K (Doster et al., 1989; Ferrand et al., 1993; Andreani et al., 1995; Fitter et al., 1997; Fitter, 1999; Bicout and Zaccai, 2001), role of hydration water (Fitter et al., 1996; Zanotti et al., 1997, 1999; Pérez et al., 1999), relationship between protein dynamics and thermal stability (Fitter and Heberle, 2000; Fitter et al., 2001; Tsai et al., 2000, 2001), solvent dependence of internal dynamics (Demmel et al., 1997; Cordone et al., 1999; Réat et al., 2000), effects of dynamics on enzyme activity (Daniel et al., 1998, 1999; Dunn et al., 2000), and analysis of vibrational modes (Cusack and Doster, 1990; Diehl et al., 1997; Andreani et al., 1997; Paciaroni et al., 1999; Bizzarri et al., 2001). Few studies have investigated the internal dynamics of the partially or completely denatured states of proteins (Receveur et al., 1997; Kataoka et al., 1999a,b; Russo et al., 2000b; Bu et al., 2000, 2001; Fitter et al., 2001; Tehei et al., 2001).

We have studied the picosecond dynamics of a globular protein in solution during heat-induced unfolding. We used

*Submitted February 5, 2002, and accepted for publication May 23, 2002.*

Dr. Russo's present address is Dept. of Bioengineering, 469 Donner Laboratory, Berkeley, CA 94720-1762, USA.

Address reprint requests to Dominique Durand, Batiment 209D, Univ Paris-Sud BP 34, 91898 Orsay Cédex, France. Tel.: +33-16-446-8083; Fax: +33-16-446-8083; E-mail: dominique.durand@lure.u-psud.fr.



0006-3495/02/11/2792/09 $2.00

a model protein, neocarzinostatin (NCS), which displays a folding pattern typical of a large protein family, the immunoglobulin fold. NCS belongs to a family of antitumor proteins of bacterial origin that contain a labile chromophore. The protein component, apo-neocarzinostatin, the object of this study, is a 113-amino-acid protein with two short disulfide bridges, located within different loops. Its structure (Adjadj et al., 1992; Kim et al., 1993) essentially consists of a seven-stranded antiparallel $\beta$-sandwich, which forms a cavity. Equilibrium unfolding experiments, with unfolding induced both thermally and chemically, were performed to characterize the unfolding pathways of NCS in terms of structure. Chemically-induced unfolding was monitored by small-angle neutron scattering, fluorescence, and differential scanning calorimetry (Russo et al., 2001). The results suggest that NCS was highly stable, and that a distribution of states existed, with various degrees of residual structure, during the unfolding process. The highly unfolded state is well described by an excluded volume chain model, as described by Russo (2000), and Russo et al. (2000a). The heat-induced unfolding of NCS was followed by small-angle x-ray scattering, in the 20–80°C temperature range (Russo, 2000; Pérez et al., 2001). It was shown that the native globular protein, in buffered $H_2O$ at pH 7 (radius of gyration $R_g = 14$ Å), begins to unfold at ~63°C and is completely unfolded at 77°C, displaying Kratky Porod chain behavior ($R_g = 26.3$ Å). The midrange temperature of the transition is $T_m \approx 68$°C. Performing the experiment in buffered $D_2O$ shifts the transition by ~3°C toward higher temperatures (Russo, 2000), giving a midrange temperature $T_m \approx 71$°C. Like chemically induced unfolding, heat-induced unfolding is complex, and may involve a collection of intermediate states leading to the fully unfolded conformation.

We report here an IQENS study of changes in the internal dynamics of NCS during thermal denaturation. We investigated four temperatures covering the range from 20°C to the midrange temperature (71°C), working with a solution in heavy water. Data were analyzed with a model that dissociates local diffusive motions and the Brownian motion of the whole protein in solution (Pérez et al., 1999). The inferred dynamic parameters are a mean of those for the various species present in the solution at each temperature.

## MATERIALS AND METHODS

### Sample preparation

Recombinant apo-NCS (mass = 11079 g/mol) was produced in *Escherichia coli* and purified as previously described (Heyd et al., 2000). The purified protein was lyophilized, dissolved in $D_2O$, and extensively dialyzed against $D_2O$ to replace the labile hydrogen atoms by deuterium. The protein was lyophilized again and dissolved in 100 mM phosphate buffer at pD 7. A first series of neutron measurements was performed at temperatures 20.8°C, 61.8°C, and 71°C, with a 58 mg/ml solution of NCS. A fresh solution (concentration, 42 mg/ml) was used for measurement at the beginning of the transition ($T = 66.3$°C), to minimize the aggregation effects due to the sample being maintained for a long period in the transition zone. We used 100 mM phosphate buffer at pD 7 for background subtraction.

### Experimental procedure

The experiment was carried out at the Orphée reactor of the Leon Brillouin Laboratory (Gif-sur-Yvette, France), using the MIBEMOL time-of-flight spectrometer. The spectrometer was operated with an incident energy of 2.27 meV, a wavevector range of $0.3 < Q < 2.0$ Å$^{-1}$ and an energy resolution half width at half maximum (HWHM) of 0.048 meV. All samples were placed in a slab 1.3 mm thick, oriented at 45° with respect to the incident beam. All samples were measured for 24 h at each temperature, to facilitate statistical analysis. All experimental spectra were corrected for the contribution made by the sample holder. They were also normalized using the vanadium standard and corrected for transmission and geometry effects. The resulting data were analyzed with the LLB programs in $(\theta, \tau)$ space, where $\theta$ is the scattering angle and $\tau$ is the neutron time of flight. Conversely, the equations used to describe the data are expressed in the $(Q, \omega)$ space, where

$$Q^2 = \left(\frac{2\pi}{\lambda_0}\right)^2 \left(2 + \frac{\omega}{\omega_0} - 2\cos(\theta)\sqrt{\frac{\omega}{\omega_0} + 1}\right)$$

$$\hbar(\omega + \omega_0) = \frac{m_n D_{SD}^2}{2\tau^2},$$

$\hbar\omega_0$ is the incident neutron energy and $\lambda_0$ the wavelength, $\hbar\omega$ is the energy transfer between the neutron and the sample, $m_n$ is the neutron mass and $D_{SD}$, the sample-to-detector distance.

### Data analysis

#### *Solvent subtraction*

The scattering function for the protein, $S_{prot}(Q, \omega)$, is obtained by subtracting the solvent contribution from that of the protein solution,

$$S_{prot}(Q, \omega) = S_{sol}(Q, \omega) - (1 - \nu)S_{buf}(Q, \omega). \quad (1)$$

$S_{sol}(Q, \omega)$ and $S_{buf}(Q, \omega)$ are the experimental scattering functions of the protein solution and of the buffer alone, respectively. The factor $\nu$ accounts for the fact that the amount of bulk solvent in the protein solution sample is less than that in the pure buffer. It corresponds to the fraction of bulk water eliminated by introduction of the protein. This value was calculated by taking into account the volume occupied by the protein and the first hydration shell. Water molecules situated within the second protein hydration shell and beyond are thought to undergo the same dynamics as pure bulk water in the picosecond time range. Given a partial specific volume of the protein of 0.72 cm$^3$g$^{-1}$, as derived following the approach of Kharakoz (1997), the value of $(1 - \nu)$ was estimated at 0.93 and 0.95 for the samples at concentrations of 58 and 42 mg/ml, respectively.

During the unfolding process, some exchangeable hydrogen atoms, which were initially buried in the native conformation and therefore not replaced by deuterium during dialysis procedure, become exposed to the solvent and are consequently exchanged. These hydrogen atoms contribute to solvent scattering via an incoherent contribution. However, this contribution has been evaluated at less than 0.7% of total solvent scattering and may be considered, as a first approximation, to be negligible.

Examples of $S_{sol}(\theta, \tau)$ spectra, $S_{buf}(\theta, \tau)$ spectra, and results of the subtraction are shown in Fig. 1.

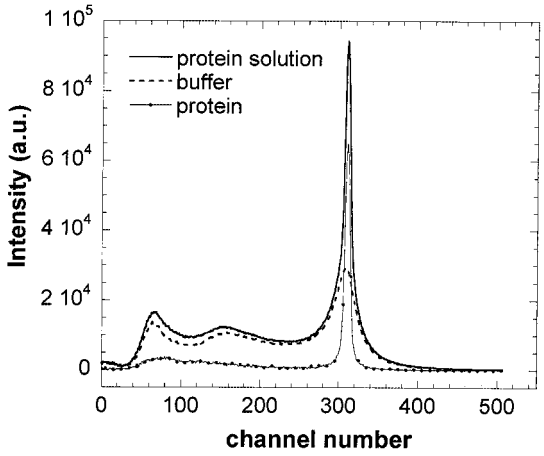


FIGURE 1 Time-of-flight experimental scattering spectra of the protein solution and the corresponding buffer at 20.8°C. The momentum transfer at the elastic peak is $Q_0 = 4\pi \sin(\theta/2)/\lambda = 1.48$ Å$^{-1}$. The resulting curve obtained after subtraction of the buffer contribution according to Eq. 1 gives the contribution of the protein alone.

### *Incoherent dynamic structure factor*

For dry or poorly hydrated protein powders, in which the macromolecules are globally confined, quasielastic neutron scattering measures the direct consequence of internal motion. In this case, the incoherent quasielastic scattering function may be described by

$$S_{\text{prot}}(Q, \omega) = \exp(-\langle u^2\rangle Q^2/3)[S_{\text{int}}(Q, \omega) + B(Q)], \quad (2)$$

where the scattering function $S_{\text{int}}(Q, \omega)$ corresponds to internal diffusive motions in the absence of vibrational modes, $\langle u^2\rangle$ stands for the mean square amplitude of vibration, and $B(Q)$ is an energy-independent background, due to the vibrational modes of lowest energy or lattice phonons (Bée, 1988). $S_{\text{int}}(Q, \omega)$ may be broken down into the sum of an elastic contribution and a quasielastic Lorentzian contribution,

$$S_{\text{int}}(Q, \omega) = A_0(Q)\delta(\omega) + (1 - A_0(Q))L(Q, \omega). \quad (3)$$

Conversely, proteins diffuse freely in solution. Thus, to investigate their internal dynamics, it is necessary to separate local motions from the Brownian motion of the whole protein in solution.

The incoherent scattering function due to translational Brownian motion is well described by a Lorentzian function, with a HWHM: $\Gamma_s(Q) = D_sQ^2$. The self-diffusion coefficient follows the Einstein relationship, $D_s = k_BT/6\pi R_H\eta$, where $R_H$ is the hydrodynamic radius of the diffusing particle, and $\eta$ is solvent viscosity. In addition to translational motions, we must also consider the rotational motions of the particle. This contribution ensures that the resulting scattering function conserves its Lorentzian shape, with $\Gamma_1(Q) = D_{\text{app}}Q^2$, where $\Gamma_1$ is the corresponding HWHM and $D_{\text{app}}$ the apparent diffusion constant, slightly higher than $D_s$ (Pérez et al., 1999). The total scattering function can now be written as

$$S_{\text{prot}}(Q, \omega) = \exp(-\langle u^2\rangle Q^2/3) \cdot L_1(Q, \omega) \otimes (S_{\text{int}}(Q, \omega) + B(Q)), \quad (4)$$

where the Lorentzian function $L_1$, of HWHM $\Gamma_1(Q)$, describes the Brownian motion of the whole protein in solution. Finally, the incoherent structure factor is described by

$$S_{\text{prot}}(Q, \omega) = \exp(-\langle u^2\rangle Q^2/3) \cdot \{L_1(Q, \omega) \otimes [A_0(Q)\delta(\omega) + (1 - A_0(Q))L_2(Q, \omega) + B(Q)]\} \otimes R(\omega). \quad (5)$$

The Lorentzian function $L_2$ describes the internal confined diffusive and reorientational motions, and provides information about the correlation time of these motions. $R(\omega)$ is the resolution function of the instrument, obtained from vanadium scattering. The variation with $Q$ of the pseudo-elastic incoherent structure factor (EISF) value, $A_0$, provides information about the geometry of the motions and about the fraction of hydrogen atoms involved in these motions. This description of the incoherent dynamic structure factor is appropriate for solutions of identical compact globular objects.

In this study, we restricted our experiments to the start of the heat-induced denaturation transition. It has been previously suggested from small-angle x-ray scattering measurements that, in the explored temperature range, the solution is a mixture of native and only partially unfolded intermediate conformations (Russo, 2000; Pérez et al., 2001). Assuming that these intermediate conformations involve residual interactions that limit backbone fluctuations, the incoherent dynamic factor structure can be written as

$$\begin{aligned} S_{\text{prot}}(Q, \omega) &= f_N * \exp(-\langle u^2\rangle_N Q^2/3)L_1^N(Q, \omega) \\ &\otimes [A_0^N(Q)\delta(\omega) + (1 - A_0^N(Q))L_2^N(Q, \omega) + B^N(Q)] \\ &+ f_I * \exp(-\langle u^2\rangle_I Q^2/3)L_1^I(Q, \omega) \\ &\otimes [A_0^I(Q)\delta(\omega) + (1 - A_0^I(Q))L_2^I(Q, \omega) + B^I(Q)]. \end{aligned} \quad (6)$$

The N and I indices refer to the native and intermediate states, respectively. $f_N$ and $f_I$ are the fractions of native and intermediate conformations. $L_1^N(Q, \omega)$ and $L_1^I(Q, \omega)$ are the Lorentzian functions arising from the global motions of the proteins. If we now assume that both native and intermediate conformations have similar rotational and translational motions, then the two Lorentzian functions, $L_1^N(Q, \omega)$ and $L_1^I(Q, \omega)$, are identical. The experimental spectra can then be analyzed with Eq. 5, in which the inferred parameters correspond to a weighted average between the native and intermediate states.

## RESULTS

Figure 2 shows two examples of the fitting procedure using Eq. 5 at two different temperatures, 20.8°C and 61.8°C, at which the protein is still in its native state. The narrow Lorentzian function corresponds to the global motion of the protein in solution, and the large Lorentzian function corresponds to internal diffusive motion.

### Brownian diffusion

Before analyzing internal dynamics, we checked that global motion was correctly deconvoluted by the fitting procedure.

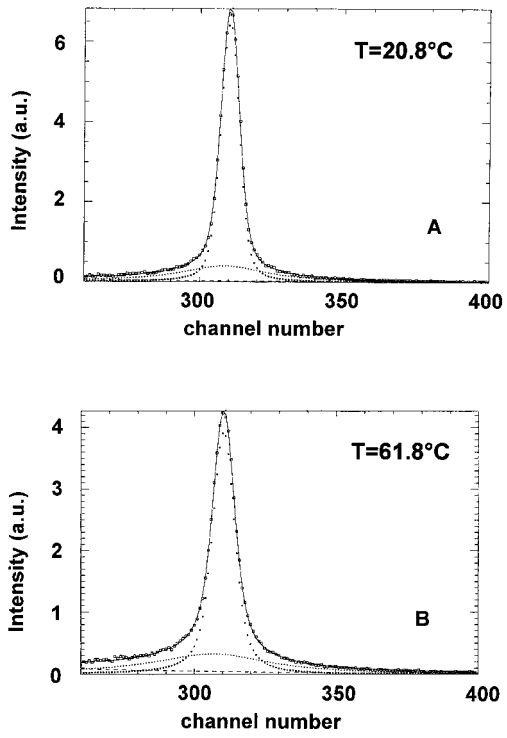


FIGURE 2 Experimental scattering spectra corrected for the solvent contribution at two temperatures (*A*) 20.8°C and (*B*) 61.8°C. The momentum transfer at the elastic peak is $Q_0 = 1.48$ Å$^{-1}$. The solid line is the fit based on Eq. 5. The two Lorentzian components are shown as dotted lines.

The apparent diffusion coefficient of the protein in solution, $D_{app}$, can be inferred from changes in the width of the narrow Lorentzian function $L_1(Q, \omega)$ with $Q$. For each temperature, changes in the HWHM of the Lorentzian function $L_1(Q, \omega)$ appear to follow a quadratic function of $Q$, as expected for a free diffusion motion, $\Gamma_1(Q) = D_{app} \cdot Q^2$ (Fig. 3). The slope of $\Gamma_1(Q)$ against $Q^2$ gives the value of the

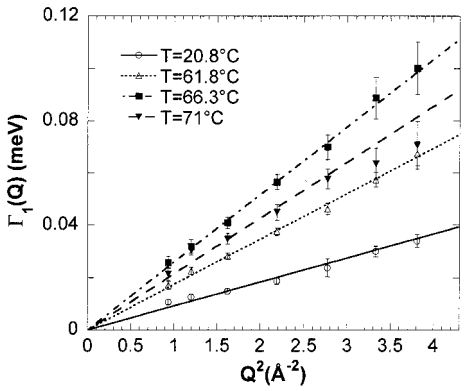


FIGURE 3 Changes in $\Gamma_1(Q)$, the HWHM of the Lorentzian component arising from the protein global motions, with $Q^2$ at each experimental temperature. The slope of $\Gamma_1$ versus $Q^2$ is indicated by a line and provides the value of $D_{app}$.

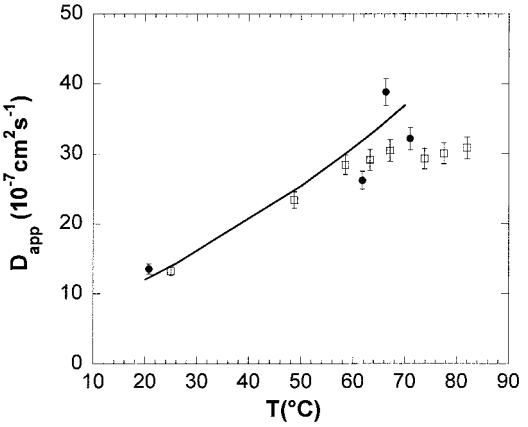


FIGURE 4 Changes in the protein apparent diffusion constant $D_{app}$ with temperature, as derived from neutron (●) and light scattering data (□). The calculated values, evaluated as described in the text, are plotted as a straight line.

apparent diffusion constant, $D_{app}$. These values are plotted in Fig. 4 as a function of temperature. For comparison, we also performed quasielastic light scattering experiments, to measure expected changes of the translation diffusion coefficient $D_{tr}$ with $T$. Light scattering was measured with a 4-mg/ml solution of NCS in $H_2O$ phosphate buffer at pH 7. For comparison with the time-of-flight results in $D_2O$, the translation diffusion coefficient values $D_{tr}$ were normalized, at each temperature, according to the ratio between the viscosities of solutions in $D_2O$ and $H_2O$, then corrected for the constant 1.27 (Pérez et al., 1999) to account for the effect of rotational motion. We also took into account the shift (≈3°C) of the transition toward higher temperatures for the $D_2O$ buffer. The inferred values are plotted in Fig. 4. We also calculated expected changes in the diffusion coefficient of the compact protein with $T$, based on the relationship

$$D_{app} = \frac{1.27 \cdot k_B T}{6\pi R_H \eta_{D_2O}(T)},$$

where

$$R_H = \sqrt{\frac{5}{3}} R_g$$

and $R_g$ is the radius of gyration of the native state, $R_g$ = 14 Å. The calculated values are plotted as a straight line in Fig. 4.

The orders of magnitude of the diffusion coefficients derived from the neutron scattering data appear to be consistent with calculated values and with values deduced from measurements of light scattering. The effect of global motions may therefore be considered to be properly deconvoluted.

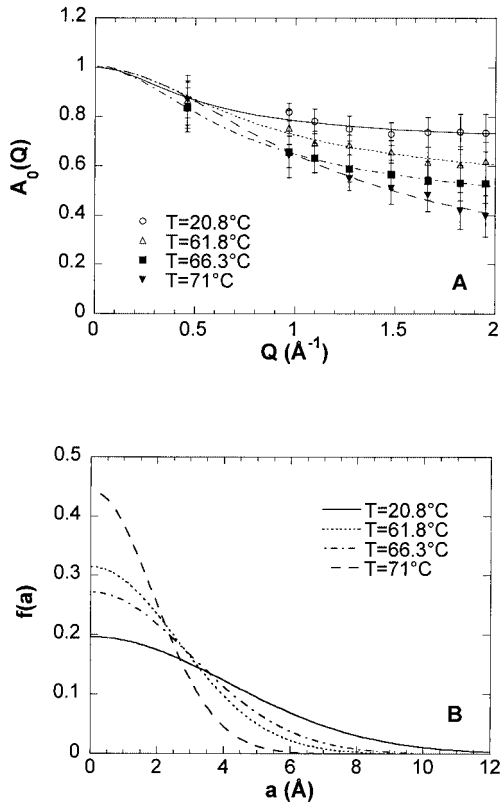


FIGURE 5 (*A*) Changes in pseudo-EISF $A_0(Q)$ at all investigated temperatures, as derived from the data analyzed with Eq. 5. The lines result from the fit of $A_0(Q)$, based on a model of free diffusion within a sphere of variable radius $a$. (*B*) Distribution of the sphere radius $f(a)$, determined by the fitting procedure, for each temperature.

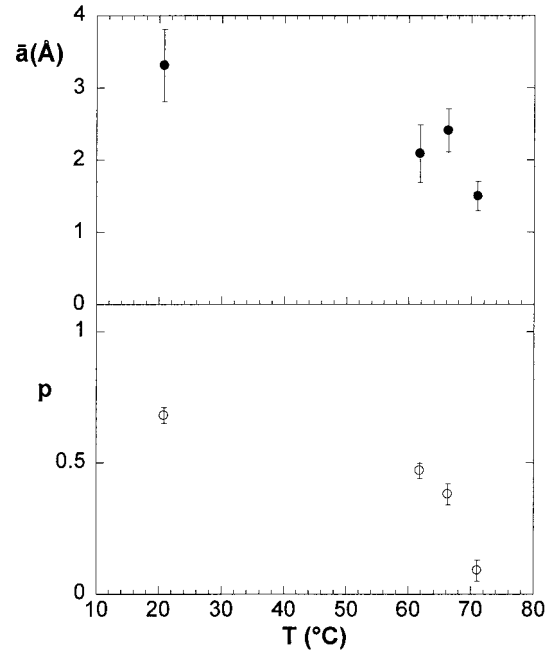


FIGURE 6 Variation of mean sphere radius, $\bar{a}$, resulting from the model of free diffusion within a sphere and of the fraction of immobile scatterers, $p$, as a function of temperature.

## Internal dynamics

### *Quasielastic amplitude*

The internal motions of a protein take place over a large time scale, and some are not detected at experimental resolutions. Scattering by these "immobile" protons makes a constant contribution to the pseudo-EISF $A_0(Q)$. To represent this effect, we introduced the parameter $p$, which remains constant with changes in $Q$, to represent the fraction of protons in the protein that are considered to be immobile. The parameter $p$ corresponds to the fraction of nonexchanged hydrogens in the protein that are only subject to motions faster than a few picoseconds or to internal diffusive motions much slower than the experimental resolution. Accordingly, $A_0$ can be written as

$$A_0(Q) = p + (1 - p)A_0'(Q), \tag{7}$$

where $A_0'(Q)$ is the pseudo-EISF of the hydrogen atoms, involved in detectable internal dynamics.

Figure 5 *A* shows the experimental $A_0(Q)$ for each temperature. The decrease in $A_0(Q)$ with $Q$ is most evident at high $Q$ as the temperature increases, which suggests that the fraction of immobile hydrogen atoms decreases as temperature increases.

The $A_0(Q)$ curves were fitted with Eq. 7 in which $A_0'(Q)$ is described according to the model of free diffusion within a sphere (Volino and Dianoux, 1980). These authors showed that free diffusion motion within a sphere of finite size implies

$$A_0'(Q) = [3j_1(Qa)/Qa]^2, \tag{8}$$

where $j_1$ is the first-order Bessel spherical function of the first kind, and $a$ is the sphere radius. To take into account the heterogeneity of proton motions within the protein, we considered a distribution function, $f(a)$ of the characteristic length $a$ rather than a unique value. The distribution $f(a)$ was assumed to be Gaussian, $f(a) = 2\sigma^{-1}(2\pi)^{-0.5}\exp(-a^2/2\sigma^2)$, with a variance $\sigma$, as the fitting parameter. The mean value of the radius $a$ is then given by $\bar{a} = \sigma(2/\pi)^{0.5}$.

The fitting curves and the radius distributions are shown in Fig. 5 for each temperature. The $f(a)$ distribution is wide enough ($\sigma \geq 1.9$) to account for typical displacements of aliphatic side-chain motions. The radius of the sphere of diffusion of a hydrogen atom along an aliphatic chain fixed at one end has been shown to increase linearly with distance from the fixed end (Carpentier et al., 1989). A value of ~2 Å was estimated for hydrogen atoms linked to the third carbon of the aliphatic chain, which is consistent with the values reported here.

Variations in mean sphere radius, $\bar{a}$, and the fraction of immobile scatterers, $p$, are shown in Fig. 6 as a function of

temperature. We found that $p$ decreased by ~30% between 20.8 and 61.8°C, whereas the protein retained its native conformation, and then underwent a more abrupt decrease when the protein started to unfold. The latter decrease in $p$ to the small value of 0.09 at 71°C shows that almost all the protons in the protein were mobile at the half-transition temperature.

The temperature dependence of $p$ before the transition can be explained if we consider that, at room temperature, the dominant contribution to internal motion is that of side chains exposed to the solvent. These side chains are free to move and to explore a large space. As temperature increases, the buried protons, most of which are within the $\beta$-sandwich, become more mobile. The observed decrease in the proportion $p$ of immobile hydrogens is thus a logical consequence.

This explanation may also account for the simultaneous decrease in mean sphere radius, $\bar{a}$, at least as long as the protein is not fully unfolded. The buried hydrogens that become mobile as temperature increases cannot explore a space as large as that explored by the exposed hydrogens. Therefore, their motion essentially decreases the mean amplitude of motion.

#### *Quasielastic width*

The Lorentzian linewidth $\Gamma_2(Q)$ seems to be almost independent of $Q$ and temperature, with a mean value of 0.25 meV. However $\Gamma_2$ determination is inaccurate and no conclusion could be deduced from this behavior.

#### *Mean square vibrational amplitude*

By the direct numerical integration of experimental data, we deduced the Debye–Waller factor, $\exp(-Q^2\langle u^2\rangle/3)$. This factor provides direct information concerning the vibrational dynamics of the protein. For each temperature, the natural logarithm of the added amplitudes of Lorentzian $L_1$ and $L_2 \otimes L_1$ varied linearly as a function of $Q^2$. The slope of the line gives the value of $\langle u^2\rangle/3$ for each temperature. The obtained values of $\langle u^2\rangle$ were between 0.12 ± 0.03 Å at 20.8°C, and 0.22 ± 0.03 Å at the half-transition temperature (71°C). Figure 7 shows the temperature dependence of $\langle u^2\rangle$. The dependence of $\langle u^2\rangle$ on temperature deviated from linearity at 66.3°C.

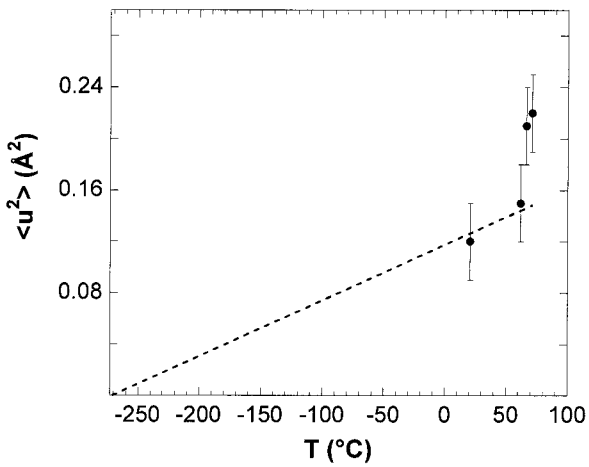


FIGURE 7 Mean square vibrational amplitude $\langle u^2\rangle$ as a function of temperature. *Dashed line*, expected change in vibrational motion amplitude $\langle u^2\rangle$ of the native NCS with temperature.

## DISCUSSION

We present here the dynamic changes that occur before and during the first steps in the heat denaturation of NCS. We observed slight but clear changes in the internal dynamics of the native NCS protein on the picosecond time scale, as a result of the increase in temperature. Moreover, all internal dynamics parameters, including the amplitude of diffusive motions, the fraction of immobile scatterers, and the mean squared vibrational amplitude, underwent stronger changes during the heat-induced unfolding.

### Brownian diffusion

Because the sample was a protein solution, we took into account in data analysis the considerable parasitic contribution of bulk solvent and Brownian motion of the protein. We estimated Brownian motion using a model developed for a native protein, which we assumed, to a first approximation, to be valid in our conditions. This enabled us to determine the protein self-diffusion constant (global translation and rotation).

One technical point concerns the width of the narrow Lorentzian function $L_1(Q, \omega)$, which takes into account the global diffusion motions of the protein in solution. The values of the HWHM, $\Gamma_1(Q)$, were generally below the experimental resolution used (0.048 meV). Thus the characteristic time of Brownian diffusion varies, as a function of $Q$, between 20 and 60 ps at a temperature of 20°C, and between 7 and 26 ps at $T = 66.3$°C, whereas the correlation time corresponding to the spectrometer resolution is 14 ps. Although any motion with a correlation time higher than the inverse of the resolution is usually considered to produce elastic scattering and is therefore ignored, it has been shown that this is not the case when dealing with the global motions of a molecule in solution (Pérez et al., 1999). In such cases, the HWHM $\Gamma_1(Q)$ can be considered as a broadening of the resolution, which is measurable even if much smaller than the resolution itself.

### Internal diffusion

To ensure that we correctly interpreted the data for $p$ (fraction of immobile protons), we analyzed the distribution of

nonexchanged hydrogen atoms on the native protein, using the Protein Data Bank file (PDB file: 1noa). The NCS protein consists of 113 amino acids, comprising a total of 1510 atoms: 778 atoms of C, N, O, and 732 H atoms. Only 172 of these hydrogen atoms are exchangeable. The remaining protons were considered to be uniformly distributed over the protein. In the case of native NCS, incoherent scattering arises predominantly from these 560 nonexchanged hydrogen atoms: 24% on the backbone, 39% on the side chains of residues involved in the $\beta$-sheet structure, and 37% on the side chains of residues in random coil structures.

We inferred from our neutron scattering analysis that the proportion $(1 - p)$ of mobile hydrogen atoms was 33% at $T = 20.8$°C. This value is very similar to the value (37%) calculated for the number of protons involved in the side chains of random coil structures. It therefore seems likely that these protons, which are very exposed to the solvent, display mainly diffusive dynamics on the picosecond time scale. According to this hypothesis, the hydrogen atoms of the backbone and the side chains involved in the beta structure are less mobile, and their dynamics have little effect.

If the temperature is increased to 61.8°C, just below the heat denaturation transition, some hydrogen atoms of the backbone and $\beta$-sheet side chains progressively acquire enough kinetic energy to diffuse locally, but with a weak amplitude because the protein is still compact. Because these protons explore a restrained spatial domain, it follows that the motions are, on average, more confined than those at ambient temperature.

This interpretation is supported by the results of $^{13}C$ NMR experiments performed at 35°C (Mispelter et al., 1995) and 50°C (E. Adjadj, personal communication) showing that, at 35°C, motions within the $\beta$-sandwich are more constrained than those within the loops, and that, at 50°C, the backbone becomes more flexible and the residues of the beta structure are less tightly constrained.

During the unfolding transition, we observed a pronounced decrease in the fraction $p$ of immobile hydrogen atoms and in the mean motion amplitude $\bar{a}$. The decrease in $p$ is easy to interpret, given that, upon partial (or total) unfolding, many more hydrogen atoms are able to diffuse than in the native, structured, state. The decrease in $\bar{a}$ at 71°C is more surprising, because we would expect relatively large amplitudes of diffusion for hydrogen atoms in an unstructured state. However, it should be noted that the value of $\bar{a}$ is strongly dependent on the $A_0$ values in the small-$Q$ range, where only one experimental point is available. In contrast, $p$ being the asymptotic value of $A_0$ at high $Q$, its value can be accurately determined. Moreover, the data analysis based on Eq. 5 may not be perfectly adequate when the population of partly unstructured intermediate state becomes important. This point has yet to be clarified.

### Debye–Waller

The Debye–Waller factor was evaluated in our approach as the ratio between the intensity scattered with an energy transfer greater than 1 meV and total intensity at a given value of $Q$. The expected change as a function of $Q^2$, $\exp(-Q^2\langle u^2\rangle/3)$, was then checked experimentally. The resulting mean square displacement, $\langle u^2\rangle$, includes only the motions corresponding to energy transfers greater than 1 meV, in particular the vibrational motions that give rise to the inelastic part of the scattered intensity. For the structured native protein, most of the diffusive motions on the picosecond time scale involve an energy transfer of less than 1 meV. Therefore, $\langle u^2\rangle$ can be considered to account only for vibrational motions. This is important because the $\langle u^2\rangle$ values usually published account both for diffusive and vibrational motions (Doster et al., 1989; Ferrand et al., 1993; Andreani et al., 1995; Réat et al., 1997, 1998) and appear to be much higher than those found here. However, it is possible to reconcile our measurements of $\langle u^2\rangle_{vibr}$ with the measurements of $\langle u^2\rangle_{total}$ reported elsewhere by extrapolating to room temperature the linear change in $\langle u^2\rangle_{total}$ with temperature before the so-called dynamic transition at ~200 K. Indeed, at temperatures lower than the transition temperature, only vibrational motions can occur, and $\langle u^2\rangle_{total}$ is equal to $\langle u^2\rangle_{vibr}$. This linear extrapolation to room temperature, as expected for motions depending on a harmonic potential, gave a value of 0.12 Å$^2$ for myoglobin (Doster et al., 1989), 0.10 Å$^2$ for superoxide dismutase (Andreani et al., 1995), and 0.15 Å$^2$ for bacteriorhodopsin (Ferrand et al., 1993). These values are similar to the value of 0.12 Å$^2$ obtained for NCS at 20.8°C.

As shown by the dashed line in Fig. 7, the values of $\langle u^2\rangle$ before the unfolding transition, at 20 and 61.8°C, are perfectly compatible with the expected linear change in vibrational motion amplitude with temperature. However, a clear departure from this linear law is observed when the protein begins to unfold, with values of $\langle u^2\rangle$ being higher than expected. One possible explanation for this behavior is the expected change in harmonic potential that occurs as soon as the protein structure begins to change dramatically. The harmonic potential of a partially or totally unfolded protein should be softer than that of the native protein, giving larger motion amplitudes. Alternatively, diffusive motions associated with energy transfers greater than 1 meV may occur in the (partially) unfolded protein. These motions would contribute to the Debye–Waller factor as an additional term to the value of $\langle u^2\rangle$.

## CONCLUSION

IQNS was used to follow changes in the internal dynamics of a small all-$\beta$ protein, NCS, during the first steps of thermal denaturation. The internal dynamics of the native fold at 21°C is consistent with diffusive motions arising

from the side chains of the polypeptide loops external to the protein core. Based on structural data, we believe that the protein backbone is slightly flexible at room temperature, and that the side chains, which are involved in the $\beta$-sandwich, are globally constrained. It is therefore not possible to detect the movement of these side chains on the time scale used. This is consistent with recent results (Dellerue et al., 2001) obtained with a globular protein, C-phycocyanin, which showed monotonic variation of dynamic parameters with distance from the protein core. If temperature increases to 61.8°C, just below the heat denaturation transition, the backbone of NCS becomes more flexible and the $\beta$-sandwich residues less constrained. Evidence for this change is provided in particular by the increasing number of protons with detectable diffusive motions. If the temperature is then increased to the half-transition temperature, almost all the protons in the protein acquire the ability to diffuse locally. To complete our analysis of dynamics during thermal unfolding, we plan to study the picosecond dynamics of the fully denatured state. In addition, experiments with different resolutions would provide additional information about the dynamics of the unfolding process.

We would like to thank Didier Lairez (LLB, Saclay) for performing the QELS experiments, Elisabeth Adjadj of the Institut Curie (Orsay) for sharing some of her results prior to publication, and Jose Teixeira (LLB, Saclay) for valuable and stimulating discussions.

This work was supported by the Commissariat à l'Energie Atomique and by the Centre National de la Recherche Scientifique.

## REFERENCES

Adjadj, E., E. Quiniou, J. Mispelter, V. Favaudon, and J. M. Lhoste. 1992. Three-dimensional solution structure of apo-neocarzinostatin from *Streptomyces carzinostaticus* determined by NMR spectroscopy. *Eur. J. Biochem.* 203:505–511.

Andreani, C., A. Deriu, A. Filabozzi, and D. Russo. 1997. Temperature dependence of inelastic dynamics of superoxide dismutase by means of neutron scattering. *Physica B.* 234–236:223–224.

Andreani, C., A. Filabozzi, F. Menzinger, A. Desideri, A. Deriu, and D. Di Cola. 1995. Dynamics of hydrogen atoms in superoxide dismutase by quasielastic neutron scattering. *Biophys. J.* 68:2519–2523.

Bai, Y., J. Chung, H. J. Dyson, and P. E. Wright. 2001. Structural and dynamic characterization of an unfolded state of poplar apoplastocyanion formed nondenaturing conditions. *Protein Sci.* 2001: 1056–1066.

Barbar, E., M. Hare, M. Makokha, G. Barany, and C. Woodward. 2001. NMR-detected order in core residues of denatured bovine pancreatic trypsin inhibitor. *Biochemistry.* 40:9734–9742.

Bée, M. 1988. Quasielastic Neutron Scattering, Principles and Applications in Solid State Chemistry, Biology and Materials Science. Adam Hilger, Bristol and Philadelphia, PA.

Bicout, D. J., and G. Zaccai. 2001. Protein flexibility from the dynamical transition: a force constant analysis. *Biophys. J.* 80:1115–1123.

Bizzarri, A. R., A. Paciaroni, C. Arcangeli, and S. Cannistraro. 2001. Low-frequency vibrational modes in proteins: a neutron scattering investigation. *Eur. Biophys. J.* 30:443–449.

Brockwell, D. J., D. A. Smith, and S. E. Radford. 2000. Protein folding mechanisms: new methods and emerging ideas. *Curr. Opin. Struct. Biol.* 10:16–25.

Bu, Z., J. Cook, and D. J. Callaway. 2001. Dynamic regimes and correlated structural dynamics in native and denatured alpha-lactalbumin. *J. Mol. Biol.* 312:865–873.

Bu, Z., D. A. Neumann, S. H. Lee, C. M. Brown, D. M. Engelman, and C. C. Han. 2000. A view of dynamics changes in the molten globule-native folding step by quasielastic neutron scattering. *J. Mol. Biol.* 301:525–536.

Carpentier, L., M. Bée, A. M. Giroud-Godquin, P. Maldivi, and J. C. Marchon. 1989. Alkyl chain motions in columnar mesophases. A quasielastic neutron scattering study of dicopper tetrapalmitate. *Mol. Phys.* 68:1367–1378.

Cordone, L., M. Ferrand, E. Vitrano, and G. Zaccai. 1999. Harmonic behavior of trehalose-coated carbon-monoxy-myoglobin at high temperature. *Biophys. J.* 76:1043–1047.

Cusack, S., and W. Doster. 1990. Temperature dependence of the low frequency dynamics of myoglobin. Measurement of the vibrational frequency distribution by inelastic neutron scattering. *Biophys. J.* 58: 243–251.

Daniel, R. M., J. L. Finney, V. Reat, R. Dunn, M. Ferrand, and J. C. Smith. 1999. Enzyme dynamics and activity: time-scale dependence of dynamical transitions in glutamate dehydrogenase solution. *Biophys. J.* 77: 2184–2190.

Daniel, R. M., J. C. Smith, M. Ferrand, S. Hery, R. Dunn, and J. L. Finney. 1998. Enzyme activity below the dynamical transition at 220 K. *Biophys. J.* 75:2504–2507.

Dellerue, S., A. J. Petrescu, J. C. Smith, and M. C. Bellissent-Funel. 2001. Radially softening diffusive motions in a globular protein. *Biophys. J.* 81:1666–1676.

Demmel, F., W. Doster, W. Petry, and A. Schulte. 1997. Vibrational frequency shifts as a probe of hydrogen bonds: thermal expansion and glass transition of myoglobin in mixed solvents. *Eur. Biophys. J.* 26: 327–335.

Diehl, M., W. Doster, W. Petry, and H. Schober. 1997. Water-coupled low-frequency modes of myoglobin and lysozyme observed by inelastic neutron scattering. *Biophys. J.* 73:2726–2732.

Doster, W., S. Cusack, and W. Petry. 1989. Dynamical transition of myoglobin revealed by inelastic neutron scattering. *Nature.* 337: 754–756.

Dunn, R. V., V. Reat, J. Finney, M. Ferrand, J. C. Smith, and R. M. Daniel. 2000. Enzyme activity and dynamics: xylanase activity in the absence of fast anharmonic dynamics. *Biochem. J.* 346:355–358.

Ferrand, M., A. J. Dianoux, W. Petry, and G. Zaccai. 1993. Thermal motions and function of bacteriorhodopsin in purple membranes: effects of temperature and hydration studied by neutron scattering. *Proc. Natl. Acad. Sci. U.S.A.* 90:9668–9672.

Fitter, J. 1999. The temperature dependence of internal molecular motions in hydrated and dry alpha-amylase: the role of hydration water in the dynamical transition of proteins. *Biophys. J.* 76:1034–1042.

Fitter, J., and J. Heberle. 2000. Structural equilibrium fluctuations in mesophilic and thermophilic alpha-amylase. *Biophys. J.* 79:1629–1636.

Fitter, J., R. Herrmann, T. Hauss, R. E. Lechner, and N. A. Dencher. 2001. Dynamical properties of $\alpha$-amylase in the folded and unfolded state: the role of thermal equilibrium fluctuations for conformational entropy and protein stabilisation. *Physica B.* 301:1–7.

Fitter, J., R. E. Lechner, G. Buldt, and N. A. Dencher. 1996. Internal molecular motions of bacteriorhodopsin: hydration-induced flexibility studied by quasielastic incoherent neutron scattering using oriented purple membranes. *Proc. Natl. Acad. Sci. U.S.A.* 93:7600–7605.

Fitter, J., R. E. Lechner, and N. A. Dencher. 1997. Picosecond molecular motions in bacteriorhodopsin from neutron scattering. *Biophys. J.* 73: 2126–2137.

Fitter, J., S. A. Verclas, R. E. Lechner, H. Seelert, and N. A. Dencher. 1998. Function and picosecond dynamics of bacteriorhodopsin in purple membrane at different lipidation and hydration. *FEBS Lett.* 433: 321–325.

Heyd, B., G. Lerat, E. Adjadj, P. Minard, and M. Desmadril. 2000. Reinvestigation of the proteolytic activity of neocarzinostatin. *J. Bacteriol.* 182:1812–1818.

Kataoka, M., M. Ferrand, A. V. Goupil-Lamy, H. Kamikubo, J. Yunoki, T. Oka, and J. C. Smith. 1999a. Dynamical and structural modifications of staphylococcal nuclease on C-terminal truncation. *Physica B.* 266: 20–26.

Kataoka, M., H. Kamikubo, J. Yunoki, F. Tokunaga, T. Kanaya, Y. Izumi, and K. Shibata. 1999b. Low energy dynamics of globular proteins studied by inelastic neutron scattering. *J. Phys. Chem. Solids.* 60: 1285–1289.

Kharakoz, D. P. 1997. Partial volumes and compressibilities of extended polypeptide chains in aqueous solution: additivity scheme and implication of protein unfolding at normal and high pressure. *Biochemistry.* 36:10276–10285.

Kim, K. H., B. M. Kwon, A. G. Myers, and D. C. Rees. 1993. Crystal structure of neocarzinostatin, an antitumor protein-chromophore complex. *Science.* 262:1042–1046.

Lehnert, U., V. Réat, M. Weik, G. Zaccai, and C. Pfister. 1998. Thermal motions in bacteriorhodopsin at different hydration levels studied by neutron scattering: correlation with kinetics and light-induced conformational changes. *Biophys. J.* 75:1945–1952.

Mispelter, J., C. Lefèvre, E. Adjadj, E. Quiniou, and V. Favaudon. 1995. Internal motions of apo-neocarzinostatin as studied by $^{13}C$ NMR methine relaxation at natural abundance. *J. Biomol. NMR.* 5:233–244.

Paciaroni, A., M. E. Stroppolo, C. Arcangeli, A. R. Bizzarri, A. Desideri, and S. Cannistraro. 1999. Incoherent neutron scattering of copper azurin: a comparison with molecular dynamics simulation results. *Eur. Biophys. J.* 28:447–456.

Pérez, J., P. Vachette, D. Russo, M. Desmadril, and D. Durand. 2001. Heat-induced unfolding of neocarzinostatin, a small all-beta protein investigated by small-angle x-ray scattering. *J. Mol. Biol.* 308:721–743.

Pérez, J., J. M. Zanotti, and D. Durand. 1999. Evolution of the internal dynamics of two globular proteins from dry powder to solution. *Biophys. J.* 77:454–469.

Réat, V., R. Dunn, M. Ferrand, J. L. Finney, R. M. Daniel, and J. C. Smith. 2000. Solvent dependence of dynamic transitions in protein solutions. *Proc. Natl. Acad. Sci. U.S.A.* 97:9961–9966.

Réat, V., H. Patzelt, M. Ferrand, C. Pfister, D. Oesterhelt, and G. Zaccai. 1998. Dynamics of different functional parts of bacteriorhodopsin: H-2H labeling and neutron scattering. *Proc. Natl. Acad. Sci. U.S.A.* 95: 4970–4975.

Réat, V., G. Zaccai, M. Ferrand, and C. Pfister. 1997. Functional dynamics in purple membrane. *In* Biological Macromolecular Dynamics. S. Cusack, H. Büttner, M. Ferrand, P. Langan, and P. Timmins, editors. Adenine Press, New York. 117–122.

Receveur, V., P. Calmettes, J. C. Smith, M. Desmadril, G. Coddens, and D. Durand. 1997. Picosecond dynamical changes on denaturation of yeast phosphoglycerate kinase revealed by quasielastic neutron scattering. *Proteins.* 28:380–387.

Russo, D. 2000. Etude structurale et dynamique de l'état natif et des états dénaturés de la néocarzinostatine, par microcalorimétrie différentielle, spectroscopies optiques et diffusion de neutrons et rayons x. PhD thesis. Université Paris-Sud, Orsay, France.

Russo, D., D. Durand, P. Calmettes, and M. Desmadril. 2001. Characterization of the denatured states distribution of neocarzinostatin by small-angle neutron scattering and differential scanning calorimetry. *Biochemistry.* 40:3958–3966.

Russo, D., D. Durand, M. Desmadril, and P. Calmettes. 2000a. Study of thermally and chemically unfolded conformations of a small $\beta$-protein by means of small-angle neutron scattering. *Physica B.* 276–278: 520–521.

Russo, D., J. Pérez, M. Desmadril, P. Calmettes, and D. Durand. 2000b. IQNS-monitored dynamical transition of a small $\beta$-protein following heat denaturation. *Physica B.* 276–278:499–500.

Smith, J. C. 2000. Inelastic and quasielastic neutron scattering: complementarity with biomolecular simulation. *In* Structure and Dynamics of Biomolecules: Neutron and Synchrotron Radiation for Condensed Matter Studies. E. Fanchon, E. Geissler, J. L. Hodeau, J. R. Regnard, and P. A. Timmins, editors. Oxford University Press, Oxford, U.K. 161–180.

Tehei, M., D. Madern, C. Pfister, and G. Zaccai. 2001. Fast dynamics of halophilic malate dehydrogenase and BSA measured by neutron scattering under various solvent conditions influencing protein stability. *Proc. Natl. Acad. Sci. U.S.A.* 98:14356–14361.

Tollinger, M., N. R. Skrynnikov, F. A. Mulder, J. D. Forman-Kay, and L. E. Kay. 2001. Slow dynamics in folded and unfolded states of an SH3 domain. *J. Am. Chem. Soc.* 123:11341–11352.

Tsai, A. M., D. A. Neumann, and L. N. Bell. 2000. Molecular dynamics of solid-state lysozyme as affected by glycerol and water: a neutron scattering study. *Biophys. J.* 79:2728–2732.

Tsai, A. M., T. J. Udovic, and D. A. Neumann. 2001. The inverse relationship between protein dynamics and thermal stability. *Biophys. J.* 81:2339–2343.

Volino, F., and A. J. Dianoux. 1980. Neutron incoherent scattering law for diffusion in a potential of spherical symmetry: general formalism and application to diffusion inside a sphere. *Mol. Phys.* 41:271–279.

Wong, K. B., J. Clarke, C. J. Bond, J. L. Neira, S. M. Freund, A. R. Fersht, and V. Daggett. 2000. Towards a complete description of the structural and dynamic properties of the denatured state of barnase and the role of residual structure in folding. *J. Mol. Biol.* 296:1257–1282.

Yao, J., J. Chung, D. Eliezer, P. E. Wright, and H. J. Dyson. 2001. NMR structural and dynamic characterization of the acid-unfolded state of apomyoglobin provides insights into the early events in protein folding. *Biochemistry.* 40:3561–3571.

Zaccai, G. 2000. Moist and soft, dry and stiff: a review of neutron experiments on hydration-dynamics-activity relations in the purple membrane of *Halobacterium salinarum*. *Biophys. Chem.* 86:249–257.

Zanotti, J. M., M. C. Bellissent-Funel, and J. Parello. 1997. Dynamics of a globular protein as studied by neutron scattering and solid-state NMR. *Physica B.* 234–236:228–230.

Zanotti, J. M., M. C. Bellissent-Funel, and J. Parello. 1999. Hydration-coupled dynamics in proteins studied by neutron scattering and NMR: the case of the typical EF-hand calcium-binding parvalbumin. *Biophys. J.* 76:2390–2411.